Interpulse TIG Welding of Titanium Alloy (Ti-6Al-4V)

Debashis Mishra[1], A. Manjunath[2] and K. Parthiban[3]
[1]Assistant Professor, CMR Technical Campus, JNTU, Hyderabad, Telangana
[2]Scientist 'F', Gas Turbine Research Establishment, DRDO, Bangalore-93
[3]Scientist 'G', Gas Turbine Research Establishment, DRDO, Bangalore-93
E-mail: debashis171@gmail.com

DOI : 10.22486/iwj/2017/v50/i4/162271

ABSTRACT

The unique properties of Titanium alloy (Ti-6Al-4V) like high strength to weight ratio, low density has made the alloy very useful material in the manufacturing of compressor blades, casings and other structural components of the gas turbine engines. The TIG welding is an arc welding process widely used in the fabrication of gas turbine engine components and its assembly. The Interpulse technique is the modified version of TIG welding process. Due to magnetic constriction and high frequency modulation of current in the interpulse technique, the arc is getting constricted which further minimizes the net heat input. In this experiment response surface optimization technique has been adopted to evaluate the effects of the input variables (main current, delta current, travel speed), on output responses (weld bead width, reinforcement height and area, penetration height and area and HAZ area). The outcome shall be beneficial in selecting suitable parameters to obtain the required shape and quality of the weld bead geometry.

Key words: Interpulse TIG Welding; Titanium alloy; Ti-6Al-4V; Weld bead width.

1.0 INTRODUCTION

Gas tungsten arc welding (GTAW) is an arc welding process in which non consumable tungsten electrode is used to produce the weld. The primary importance of such commonly used welding technique lies with economy and its potential capability towards the joining of various metals and their alloys of thin sections such as most of the steels including stainless steel, aluminum, titanium and nickel based superalloys. The most effective feature of this technique is the intense heat source. The TIG welding process is frequently used in the manufacturing of gas turbine engine components. The elevated Strength-to-Density Ratio (high structural efficiency), low Density (roughly half the weight of steel, nickel and copper alloys) and excellent elevated Temperature properties (up to 650°C) made the Ti-6Al-4V titanium alloy most desirable material for the successful use in the manufacturing of the blades, gas turbine engines and air frame structures and other different components which demand high levels of reliable performance. A constant current AC and DC welding power supply is generally used to produce energy which leads to high heat input. This problem is encountered by the pulsing the current to a higher and a lower value. This pulse increases the energy in the arc and melts off an amount of filler rod to allow correct penetration and then when pulse ceases there is left only background current to keep the arc ionized and the weld metal freezes. The weld thus progresses as a series of overlapping spot welds. This method is very advantageous for thin and medium sections of welding. Pulsed-arc transfer means that the weld metal is projected across the gap at high current, but the mean welding current remains relatively low [1-5].

Further development in pulsing of current brought up the Interpulse technique (IPTIG) named as Interpulse gas tungsten constricted arc welding process. It uses magnetic constriction and high frequency (20,000 Hz) modulation of the arc waveform to produce a constricted arc, which greatly reduces the net heat input. The principle of the Interpulse TIG welding is the strength of the electric field is directly proportional to the rate of change of magnetic field. The well-known statistical technique response surface methodology is used to model the experiment and also to optimize the welding process parameters to identify the effects of process parameters on the responses [1,6-10].

2.0 OBJECTIVE OF THE EXPERIMENT

The weld bead terms is influenced by the welding parameters like arc current, arc voltage and arc travel speed. The weld bead geometry given below in **Fig. 1** is specified by the terms like weld bead width, reinforcement area and height, penetration area and height, heat affected zone area [5]. The objective of this experiment is to know the effect of the magnetic constriction of the arc on the weld bead geometry and to evaluate and establish a relationship between the weld bead geometry terms with the input parameters.

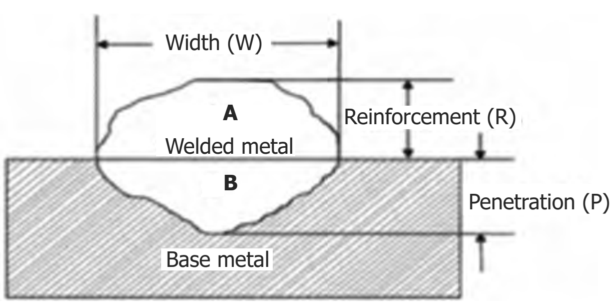

Fig. 1 : Weld bead geometry

2.1 Selection of the process variables and their limits

The Interpulse TIG welding input parameters are taken for the experimentation as main current, background current, delta current, delta frequency fixed at (20 KHz), pre purging and post purging gas fixed at 2sec and 5sec simultaneously and travel speed (mm/min). Numbers of preliminary experiments were carried out using 1.2 mm thick rolled sheets of Titanium alloy (Ti-6Al-4V) to find feasible working limits of Interpulse TIG welding parameters. Visual inspection of the reinforcement height, weld bead and penetration were inspected to identify the working limits of welding parameters which is given below in the **Table 2**. Fluorescent particle inspection was also used to identify the working limits of the welding parameters and leading to following observations.

1. If the main current was less than 60 Amps, then incomplete penetration and lack of fusion was observed. For the main current more than 80 A, undercut and spatter was observed because of the excess penetration.
2. The wider bead was observed if the delta current was less than 15 Amps. And if above 35 Amps because of high constriction of arc it was found difficulties in controlling the arc.
3. Slower welding speed 70 mm/min, undercut was observed due to high heat input. For welding speed higher than 122 mm/min there will be lack of fusion and lack of penetration.
4. The additional process parameter background current 'I_b' was maintained within 1 Amps to 14 Amps to keep the arc alive, tabulated below in **Table 3**.
5. The penetration weld was produced with the main current greater than the Interpulse or delta current.
6. The upper and lower limits of the parameters were coded as +1.682 and -1.682 respectively [10]. Due to wide ranges of factors three factors at five levels of rotatable central composite design matrix were selected to draw the experimental conditions using the JMP statistical software.

3.0 CONDUCTING THE EXPERIMENT

Pre welding cleaning: The Ti-6Al-4V sheet surfaces were polished and all the burrs are removed using grinding wheel and emery paper. Then the sheets were vapour degreased for the removal of oil and grease. Finally the sheets were followed for acid pickling with 30% to 40% of Nitric acid and balanced with distilled water. Again prior to welding acetone cleaning is followed up using a lint free cloth.

Welding: With the help of an appropriate fixture two sheets of Ti-6Al-4V are clamped and then tack welded to avoid mismatch between the two sheets. Experiments were performed on IE175i HMS (heat management system) narrow bead Interpulse TIG welding machine.

1. Work piece material: Titanium alloy Ti-6Al-4V sheets of 150×150×1.2 (mm) size, compositions are shown below in Table 1.

2. Electrode used: Thoriated tungsten of 1.6 mm.
3. Type of joint: Square butt joint.
4. The pure shielding argon gas (99.996%) is used to prevent weld from atmospheric contaminations. The experimental setup is shown in **Fig. 1.**

Fig. 2 : Experimental setup - (1) Argon Gas cylinder (2) IPTIG Welding Machine (3) Welding Fixture

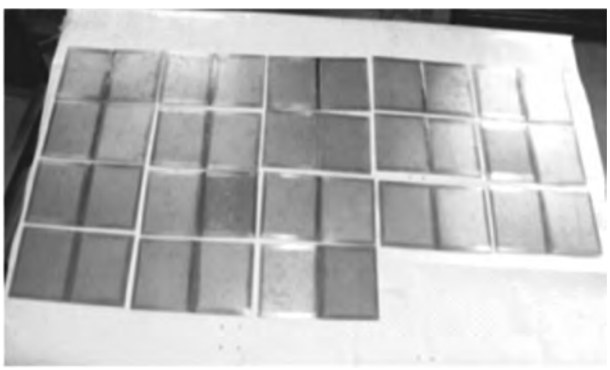

Fig. 3 : IPTIG 18 welded Ti-6Al-4V sheets

3.1 Preparation of specimens

Metallographic specimens of 10×10 mm length were extracted from each welded coupons by the laser cutting. The steps involved in the preparation of the metallographic sample are mounting, grinding, polishing and etching. Kroll's reagent was used to etch the specimens.

3.2 Measurement of the responses

The etched samples were placed under the microscope and the images of all samples were taken in 50X magnification. The weld bead geometry has been studied and bead width, reinforcement area and height, penetration area and height, heat affected zone area were measured. Heat input is calculated and tabulated below in **Table 3**. The Olympus GX71 is an inverted microscope used for microscopic observations. Biovis materials plus V4.56 software is used for the image analysis, in which images were taken and measurement has been done by drawing a polygon.

3.3 Developing empirical relationship

In this study, the response function of the joint "Y", are functions of main current (I_m), Interpulse or delta current (I_d), welding speed (S) and it can be expressed as :

$$Y = f(I_m, I_d, S) \quad (1)$$

The second order polynomial (regression) equation that represents the response surface "Y" is :

$$Y = b_o + \Sigma\, b_i x_i + \Sigma\, b_{ii} x_i^2 + \Sigma\, b_{ij} x_i x_j \quad (2)$$

Considering the above mentioned three process parameters, the selected polynomial could be expressed as:

$$\sigma = b_0 + b_1(I_m) + b_2(I_d) + b_3(S) + b_{11}(I_m^2) + b_{22}(I_d{}^2) + b_{33}(S^2) + b_{12}(I_m I_d) + b_{13}(I_m S) + b_{23}(I_d S) \quad (3)$$

Where b_o is the average of all responses and b_i, b_{ii}, b_{ij} are the coefficients that depend on the main and interaction effect of the process parameters. The obtained regression expressions of responses are given below in the equations from 4 to 8.

Table 1 : Chemical composition (wt %) of Titanium (Ti-6Al-4V)

C	Fe	N	O	Al	V	Ti
0.08	0.25	0.05	0.20	5.50-6.75	3.5-4.5	Bal.

Table 2 : IPTIG parameters & their feasible working ranges

Sl. No.	Parameters	-1.682	-1	0	1	1.682
1	Main current (Amps) 'I_m'	61	65	70	75	78
2	Delta current (Amps) 'I_d'	16	20	25	30	33
3	Welding speed (mm/min) 'S'	70	80	95	110	120

Table 3 : Design matrix, experimental outputs, BW- bead width, RH and RA -reinforcement height and area, PA and PH –penetration area and height, I_b- base current

Sl. No.	Expt. Pattern	I_m A	I_d A	S mm/ min	BW mm	RH mm	RS mm^2	PA mm^2	PH mm	HAZ area mm^2	Heat input j/mm	I_b A
1	−,−,−	65	20	80	3.94	0.11	0.47	4.47	1.25	0.96	183	4
2	−,−,+	65	20	110	3.82	0.121	0.411	4.3	1.36	0.98	143	12
3	−,+,−	65	30	80	4.47	0.098	0.336	3.97	1.32	1.02	217	4
4	-,+,+	65	30	110	4.27	0.124	0.32	3.68	1.25	0.93	168	12
5	+,-,-	75	20	80	4.42	0.131	0.412	3.69	1.28	1.05	201	4
6	+,-,+	75	20	110	4.53	0.095	0.387	3.81	1.37	0.97	156	12
7	+,+,-	75	30	80	4.25	0.164	0.48	4.78	1.40	1.09	234	4
8	+,+,+	75	30	110	4.14	0.14	0.42	4.80	1.35	0.93	180	12
9	a,0,0	61	25	95	4.09	0.111	0.326	3.79	1.25	0.93	170	8
10	A,0,0	78	25	95	4.36	0.15	0.398	4.01	1.35	1.03	207	8
11	0,a,0	70	16	95	4.19	0.131	0.496	4.29	1.38	0.99	158	8
12	0,A,0	70	33	95	4.26	0.16	0.423	4.49	1.37	1.0	204	8
13	0,0,a	70	25	70	4.4	0.118	0.412	4.11	1.26	1.08	235	1
14	0,0,A	70	25	120	4.21	0.11	0.34	3.90	1.30	1	151	14
15	0,0,0	70	25	95	3.96	0.151	0.359	3.89	1.28	1.22	181	8
16	0,0,0	70	25	95	4.02	0.149	0.354	3.86	1.27	1.19	181	8
17	0,0,0	70	25	95	3.98	0.154	0.371	3.93	1.26	1.25	181	8
18	0,0,0	70	25	95	4.05	0.157	0.368	3.96	1.28	1.2	181	8

$$\textbf{Weld bead width} = \Big[4.0025 + \Big[0.1 \times \Big[\frac{[I_m - 70]}{5}\Big]\Big] + \Big[0.044 \times \Big[\frac{[I_d - 25]}{5}\Big]\Big] + \Big[-0.046 \times \Big[\frac{[S-95]}{15}\Big]\Big] + \Big[\frac{[I_m - 70]}{5}\Big] \times \Big[\Big[\frac{[I_d - 25]}{5}\Big] \times (-0.192)\Big] + \Big[\frac{[I_m - 70]}{5}\Big] \times \Big[\Big[\frac{[S-95]}{15}\Big] \times 0.04\Big] + \Big[\frac{[I_d - 25]}{5}\Big] \times \Big[\Big[\frac{[S-95]}{15}\Big] \times (-0.037)\Big] + \Big[\Big[\frac{[I_m^2 - 70]}{5}\Big] \times 0.072\Big] + \Big[\Big[\frac{[I_d^2 - 25]}{5}\Big] \times 0.071\Big] + \Big[\Big[\frac{[S^2 - 95]}{15}\Big] \times 0.1\Big]\Big] \quad (4)$$

$$\textbf{Reinforcement Height} = \Big[0.15 + \Big[0.0096 \times \Big[\frac{[I_m - 70]}{5}\Big]\Big] + \Big[0.008 \times \Big[\frac{[I_d - 25]}{5}\Big]\Big] + \Big[-0.002 \times \Big[\frac{[S-95]}{15}\Big]\Big] + \Big[\frac{[I_m - 70]}{5}\Big] \times \Big[\Big[\frac{[I_d - 25]}{5}\Big] \times 0.01\Big] + \Big[\frac{[I_m - 70]}{5}\Big] \times \Big[\Big[\frac{[S-95]}{15}\Big] \times (-0.012)\Big] + \Big[\frac{[I_d - 25]}{5}\Big] \times \Big[\Big[\frac{[S-95]}{15}\Big] \times 0.0033\Big] + \Big[\Big[\frac{[I_m^2 - 70]}{5}\Big] \times (-0.0086)\Big] + \Big[\Big[\frac{[I_d^2 - 25]}{5}\Big] \times (-0.0035)\Big] + \Big[\Big[\frac{[S^2 - 95]}{15}\Big] \times (-0.015)\Big]\Big] \quad (5)$$

$$\textbf{Reinforcement Area} = \Big[0.36 + \Big[0.02 \times \Big[\frac{[I_m - 70]}{5}\Big]\Big] + \Big[-0.01 \times \Big[\frac{[I_d - 25]}{5}\Big]\Big] + \Big[-0.02 \times \Big[\frac{[S-95]}{15}\Big]\Big] + \Big[\frac{[I_m - 70]}{5}\Big] \times \Big[\Big[\frac{[I_d - 25]}{5}\Big] \times 0.04\Big] + \Big[\frac{[I_m - 70]}{5}\Big] \times \Big[\Big[\frac{[S-95]}{15}\Big] \times (-0.001)\Big] + \Big[\frac{[I_d - 25]}{5}\Big] \times \Big[\Big[\frac{[S-95]}{15}\Big] \times 0.001\Big] + \Big[\Big[\frac{[I_m^2 - 70]}{5}\Big] \times 0.001\Big] + \Big[\Big[\frac{[I_d^2 - 25]}{5}\Big] \times 0.033\Big] + \Big[\Big[\frac{[S^2 - 95]}{15}\Big] \times 0.005\Big]\Big] \quad (6)$$

$$\textbf{Penetration Area} = \Big[3.904 + \Big[0.077 \times \Big[\frac{[I_m - 70]}{5}\Big]\Big] + \Big[0.11 \times \Big[\frac{[I_d - 25]}{5}\Big]\Big] + \Big[-0.048 \times \Big[\frac{[S-95]}{15}\Big]\Big] + \Big[\frac{[I_m - 70]}{5}\Big] \times \Big[\Big[\frac{[I_d - 25]}{5}\Big] \times 0.399\Big] + \Big[\frac{[I_m - 70]}{5}\Big] \times \Big[\Big[\frac{[S-95]}{15}\Big] \times 0.076\Big] + \Big[\frac{[I_d - 25]}{5}\Big] \times \Big[\Big[\frac{[S-95]}{15}\Big] \times (-0.027)\Big] + \Big[\Big[\frac{[I_m^2 - 70]}{5}\Big] \times 0.015\Big] + \Big[\Big[\frac{[I_d^2 - 25]}{5}\Big] \times 0.186\Big] + \Big[\Big[\frac{[S^2 - 95]}{15}\Big] \times 0.052\Big]\Big] \quad (7)$$

$$\textbf{Penetration Height} = \Big[1.276 + \Big[0.03 \times \Big[\frac{[I_m - 70]}{5}\Big]\Big] + \Big[0.006 \times \Big[\frac{[I_d - 25]}{5}\Big]\Big] + \Big[0.012 \times \Big[\frac{[S-95]}{15}\Big]\Big] + \Big[\frac{[I_m - 70]}{5}\Big] \times \Big[\Big[\frac{[I_d - 25]}{5}\Big] \times 0.017\Big] + \Big[\frac{[I_m - 70]}{5}\Big] \times \Big[\Big[\frac{[S-95]}{15}\Big] \times 0.0006\Big] + \Big[\frac{[I_d - 25]}{5}\Big] \times \Big[\Big[\frac{[S-95]}{15}\Big] \times (-0.039)\Big] + \Big[\Big[\frac{[I_m^2 - 70]}{5}\Big] \times 0.011\Big] + \Big[\Big[\frac{[I_d^2 - 25]}{5}\Big] \times 0.035\Big] + \Big[\Big[\frac{[S^2 - 95]}{15}\Big] \times 0.003\Big]\Big] \quad (8)$$

$$\textbf{HAZ Area} = \Big[1.214 + \Big[0.016 \times \Big[\frac{[I_m - 70]}{5}\Big]\Big] + \Big[-0.003 \times \Big[\frac{[I_d - 25]}{5}\Big]\Big] + \Big[-0.032 \times \Big[\frac{[S-95]}{15}\Big]\Big] + \Big[\frac{[I_m - 70]}{5}\Big] \times \Big[\Big[\frac{[I_d - 25]}{5}\Big] \times (-0.001)\Big] + \Big[\frac{[I_m - 70]}{5}\Big] \times \Big[\Big[\frac{[S-95]}{15}\Big] \times (-0.021)\Big] + \Big[\frac{[I_d - 25]}{5}\Big] \times \Big[\Big[\frac{[S-95]}{15}\Big] \times (-0.023)\Big] + \Big[\Big[\frac{[I_m^2 - 70]}{5}\Big] \times (-0.081)\Big] + \Big[\Big[\frac{[I_d^2 - 25]}{5}\Big] \times (-0.075)\Big] + \Big[\Big[\frac{[S^2 - 95]}{15}\Big] \times (-0.064)\Big]\Big] \quad (9)$$

3.4 Adequacy of developed relationship

The adequacy of the developed relationship was investigated using the analysis of variance technique (ANOVA). It is understood that the developed relationship is adequate at 95% confidence level. The terms which has values of 'probability > F' is less that 0.05, the relationship term will be considered as significant term. An R-Square closer to 1 indicates better fit the data than does an R-Square closer to 0. The lack of fit is insignificant in all response models which describes the relational model fits the experimental data well [3,4,6,7,9]. The summary of fit, analysis of variance, lack of fit, effects test for the response models are tabulated in the **Table 4** through **Table 7**. Correlation graphs between actual and predicted response values of the said responses are presented below in the **Fig. 4**.

Table 4 : Summary of fit for response models

Models	BW	RH	RA	PA	PH	HAZ area
RSquare	0.98	0.98	0.98	0.98	0.99	0.98
RSquare Adjust	0.95	0.95	0.95	0.97	0.98	0.96
Root mean square error	0.04	0.004	0.01	0.059	0.007	0.021
Mean of response	4.18	0.13	0.39	4.097	1.31	1.046
Observations	18	18	18	18	18	18

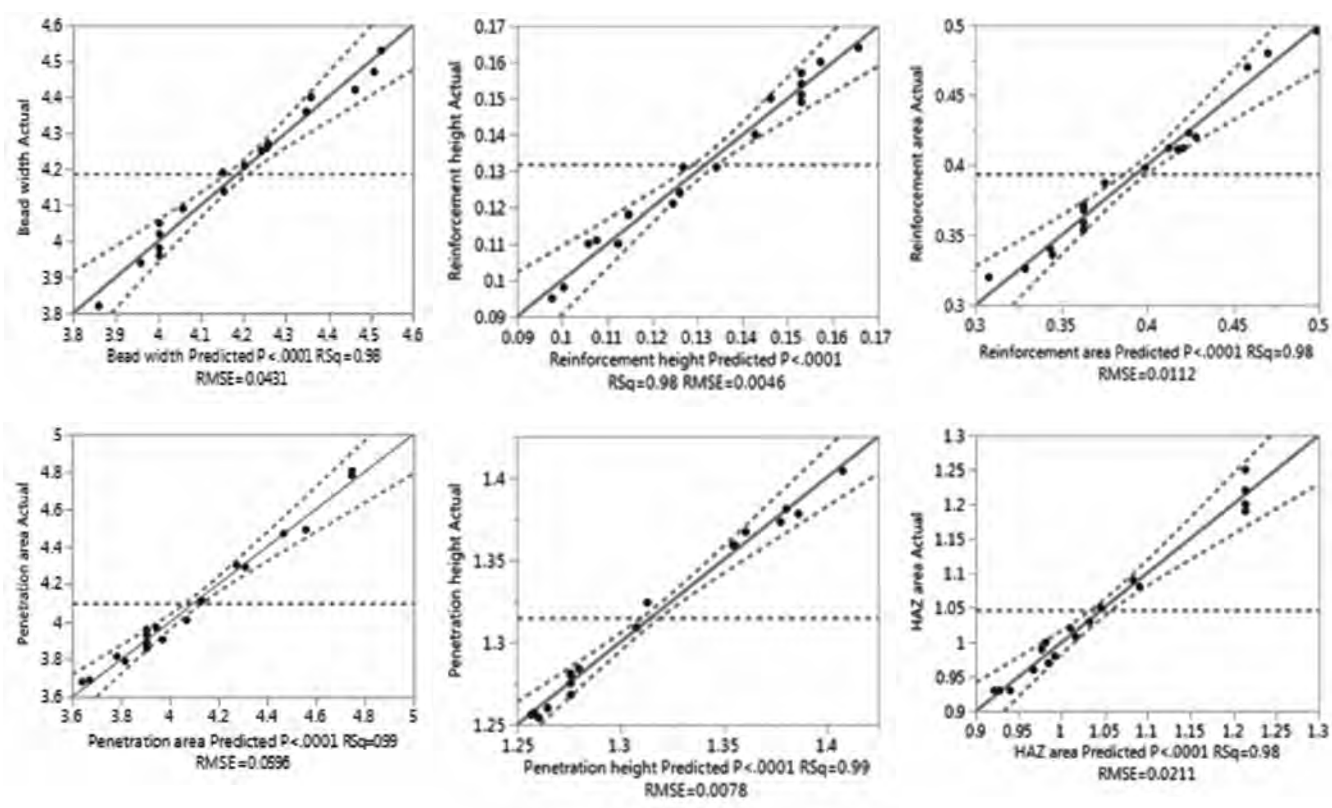

Fig. 4 : Correlation graphs between actual and predicted values of responses; bead width, re-inforcement height, reinforcement area, penetration area, penetration height, HAZ area

Table 5 : The analysis of variance for the response models; weld bead width, re-inforcement height and area, penetration area and height, HAZ area

Source	Degrees of Freedom	Sum of Squares	Mean Square	F Ratio	Whether significant/not
Model	9	0.677	0.075	40.4599	
Error	8	0.014	0.0018	**Prob > F**	
Corrected total	17	0.692		< .0001*	Yes
Source	**Degrees of Freedom**	**Sum of Squares**	**Mean Square**	**F Ratio**	**Whether significant/not**
Model	9	0.0080997	0.000900	41.8631	
Error	8	0.0001719	0.000021	**Prob > F**	
Corrected total	17	0.0082717		<.0001*	Yes
Source	**Degrees of Freedom**	**Sum of Squares**	**Mean Square**	**F Ratio**	**Whether significant/not**
Model	9	0.0454952	0.005055	40.2282	
Error	8	0.0010052	0.000126	**Prob > F**	
Corrected total	17	0.0465005		<.0001*	Yes
Source	**Degrees of Freedom**	**Sum of Squares**	**Mean Square**	**F Ratio**	**Whether significant/not**
Model	9	2.028733	0.225415	63.4697	
Error	8	0.028412	0.003552	**Prob > F**	
Corrected total	17	2.057146		<.0001*	Yes
Source	**Degrees of Freedom**	**Sum of Squares**	**Mean Square**	**F Ratio**	**Whether significant/not**
Model	9	0.046559	0.005173	85.1970	
Error	8	0.000485	0.000061	**Prob > F**	
Corrected total	17	0.047044		<.0001*	Yes
Source	**Degrees of Freedom**	**Sum of Squares**	**Mean Square**	**F Ratio**	**Whether significant/not**
Model	9	0.181430	0.020159	45.4812	
Error	8	0.003545	0.000443	**Prob > F**	
Corrected total	17	0.184976		<.0001*	Yes

Table 6 : Lack of Fit for response models; weld bead width, reinforcement height and area, penetration area and height, HAZ area

Source	Degrees of Freedom	Sum of Squares	Mean Square	F Ratio
Lack of Fit	5	0.01	0.002	1.232
Pure Error	3	0.005	0.001	**Prob > F**
Total Error	8	0.015		**0.4603* (Insignificant)**
Source	**Degrees of Freedom**	**Sum of Squares**	**Mean Square**	**F Ratio**
Lack of Fit	5	0.00013523	0.000027	2.2079
Pure Error	3	0.00003675	0.000012	**Prob > F**
Total Error	8	0.00017198		**0.2734* (Insignificant)**
Source	**Degrees of Freedom**	**Sum of Squares**	**Mean Square**	**F Ratio**
Lack of Fit	5	0.00081927	0.000164	2.6428
Pure Error	3	0.00018600	0.000062	**Prob > F**
Total Error	8	0.00100527		**0.2268* (Insignificant)**
Source	**Degrees of Freedom**	**Sum of Squares**	**Mean Square**	**F Ratio**
Lack of Fit	5	0.02261227	0.004522	2.3392
Pure Error	3	0.00580000	0.001933	**Prob > F**
Total Error	8	0.02841227		**0.2578* (Insignificant)**
Source	**Degrees of Freedom**	**Sum of Squares**	**Mean Square**	**F Ratio**
Lack of Fit	5	0.00037977	0.000076	2.1496
Pure Error	3	0.00010600	0.000035	**Prob > F**
Total Error	8	0.00048577		**0.2809* (Insignificant)**
Source	**Degrees of Freedom**	**Sum of Squares**	**Mean Square**	**F Ratio**
Lack of Fit	5	0.00144589	0.000289	0.4131
Pure Error	3	0.00210000	0.000700	**Prob > F**
Total Error	8	0.00354589		**0.8182* (Insignificant)**

Table 7 : Effect Tests for response models; weld bead width, reinforcement height and area, penetration area and height, HAZ area, DF-degrees of freedom

Source	DF	Sum of Squares	F Ratio	Prob > F	Whether significant or not
I_m (65,75)	1	0.13635860	73.28	<.0001*	Yes
I_d (20, 30)	1	0.02730591	14.67	0.0050*	Yes
S (80, 110)	1	0.02990246	16.07	0.0039*	Yes
$I_m \times I_d$	1	0.29645000	159.33	<.0001*	Yes
$I_m \times$ S	1	0.01280000	6.87	0.0305*	Yes
$I_d \times$ S	1	0.01125000	6.046	0.0394*	Yes
I_m^2	1	0.06987440	37.55	0.0003*	Yes
I_d^2	1	0.06675713	35.8795	0.0003*	Yes
S^2	1	0.12329055	66.2641	<.0001*	Yes
Source	**DF**	**Sum of Squares**	**F Ratio**	**Prob > F**	**Significant or not**
I_m (65, 75)	1	0.00126090	58.6517	<.0001*	Yes
I_d (20, 30)	1	0.00092519	43.0357	0.0002*	Yes
S (80, 110)	1	0.00009739	4.5300	0.0660	No
$I_m \times I_d$	1	0.00094613	44.0097	0.0002*	Yes
$I_m \times$ S	1	0.00117612	54.7084	<.0001*	Yes
$I_d \times$ S	1	0.00009113	4.2388	0.0735	No
I_m^2	1	0.00099063	46.079	0.0001*	Yes
I_d^2	1	0.00016145	7.5098	0.0254*	Yes
S^2	1	0.00289598	134.709	<.0001*	Yes
Source	**DF**	**Sum of Squares**	**F Ratio**	**Prob > F**	**Significant or not**
I_m (65, 75)	1	0.00586906	46.7064	0.0001*	Yes
I_d (20, 30)	1	0.00313372	24.9383	0.0011*	Yes
S (80, 110)	1	0.00578361	46.0263	0.0001*	Yes
$I_m \times I_d$	1	0.01328450	105.719	<.0001*	Yes
$I_m \times$ S	1	0.00001250	0.0995	0.7605	No
$I_d \times$S	1	0.00000800	0.0637	0.8072	No
I_m^2	1	0.00001512	0.1203	0.7376	No
I_d^2	1	0.01481140	117.87	<.0001*	Yes
S^2	1	0.00036917	2.9379	0.1249	No
Source	**DF**	**Sum of Squares**	**F Ratio**	**Prob > F**	**Significant or not**
I_m (65, 75)	1	0.0822570	23.1610	0.0013*	Yes
I_d (20, 30)	1	0.1661746	46.7895	0.0001*	Yes
S (80, 110)	1	0.0311680	8.7759	0.0181*	Yes
$I_m \times I_d$	1	1.2784005	359.957	<.0001*	Yes
$I_m \times$ S	1	0.0465125	13.096	0.0068*	Yes
$I_d \times$ S	1	0.0061605	1.7346	0.2243	No

I_m^2	1	0.0033042	0.9304	0.3630	No
I_d^2	1	0.4585253	129.106	<.0001*	Yes
S^2	1	0.0338186	9.5223	0.0150*	Yes
Source	**DF**	**Sum of Squares**	**F Ratio**	**Prob > F**	**Significant or not**
I_m (65, 75)	1	0.01226445	201.98	<.0001*	Yes
I_d (20, 30)	1	0.00054433	8.9645	0.0172*	Yes
S (80, 110)	1	0.00225062	37.065	0.0003*	Yes
$I_m \times I_d$	1	0.00255613	42.096	0.0002*	Yes
$I_m \times$ S	1	0.00000313	0.0515	0.8262	No
$I_d \times$ S	1	0.01256112	206.86	<.0001*	Yes
I_m^2	1	0.00187452	30.871	0.0005*	Yes
I_d^2	1	0.01688014	277.99	<.0001*	Yes
S^2	1	0.00016700	2.7503	0.1358	No
Source	**DF**	**Sum of Squares**	**F Ratio**	**Prob > F**	**Significant or not**
I_m (65, 75)	1	0.00364801	8.2304	0.0209*	Yes
I_d (20, 30)	1	0.00015667	0.3535	0.5686	No
S (80, 110)	1	0.01449918	32.7121	0.0004*	Yes
$I_m \times I_d$	1	0.00001250	0.0282	0.8708	No
$I_m \times$ S	1	0.00361250	8.1503	0.0213*	Yes
$I_d \times$ S	1	0.00451250	10.1808	0.0128*	Yes
I_m^2	1	0.08726702	196.886	<.0001*	Yes
I_d^2	1	0.07468023	168.488	<.0001*	Yes
S^2	1	0.05034553	113.586	<.0001*	Yes

4.0 OPTIMIZATION OF IPTIG WELDING

The response surface methodology is a statistical technique used for the experimentation and optimization of IPTIG welding process parameters to achieve the optimum condition.

4.1 Contour plot reports

The contour plots are topographical images useful for establishing the desirable response values and operating condition in a rectangular co-ordinate system. The contour plots represents the relationship in two dimensions, with factors main current, delta current and welding speed in X and Y axis and the response values by contours shown below in the **Fig. 5**.

4.2 Response surface reports

An Iso-response-surface is a three dimensional representation of three process variables in X, Y and Z axis, optimal point in space and predicted formula on surface. The second order model with square terms described by several shaped response surfaces. The stationary point of the response surface can be minimum, maximum or saddle point (minimax). In the cases of responses weld bead width, reinforcement height and area, penetration height and area, the stationary point is at saddle point. Whereas in the case of the response HAZ area the stationary point of the response surface is maximum. The predicted value at solution is weld bead width 4.11mm, reinforcement height 0.11mm, reinforcement area 0.35mm^2, penetration area 3.88mm^2, penetration height 1.25mm, HAZ area 1.22mm^2. The optimized parameter is main current 70Amps, delta current 25Amps and welding speed 95mm/min. Moreover the saddle point surface describes the axes are not in standard orientation, the origin (0, 0) is visible and there is a clear visualization of increase or decrease in function while moving to different quadrants on the surface. The isometric response surface plot of responses weld bead width, reinforcement height and area, penetration height and area, HAZ area are shown in the **Fig. 6** and **Fig. 7** respectively.

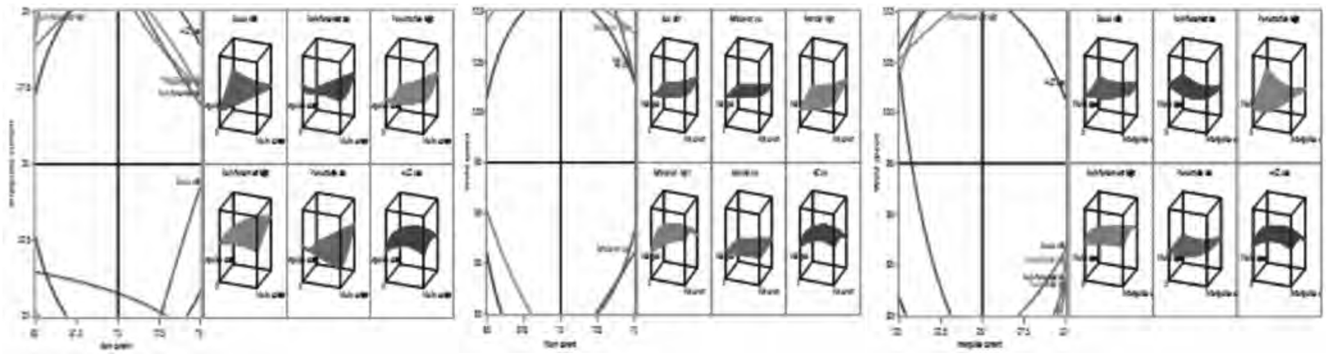

Fig. 5 : Contour plots in terms of factors and w.r.t. responses

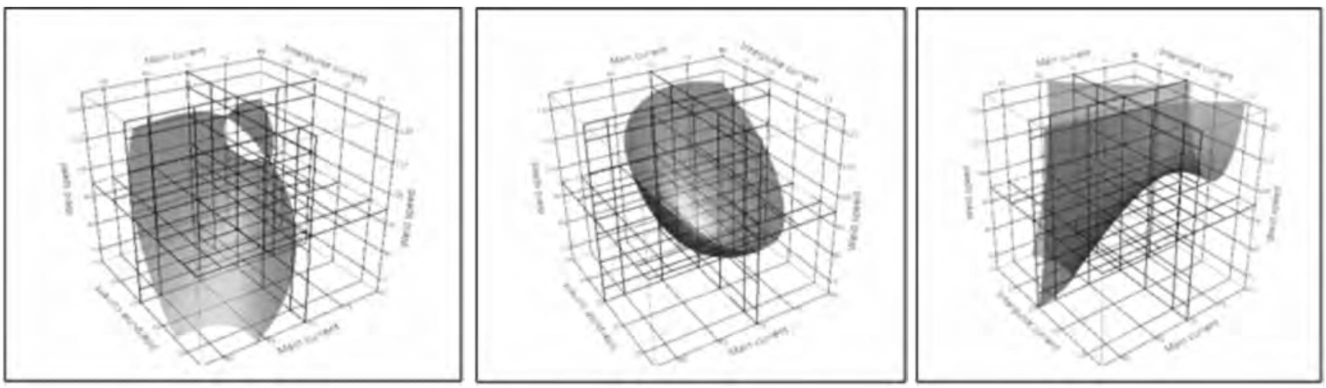

Fig. 6 : Isosurface plot of responses - bead width, reinforcement height, reinforcement area

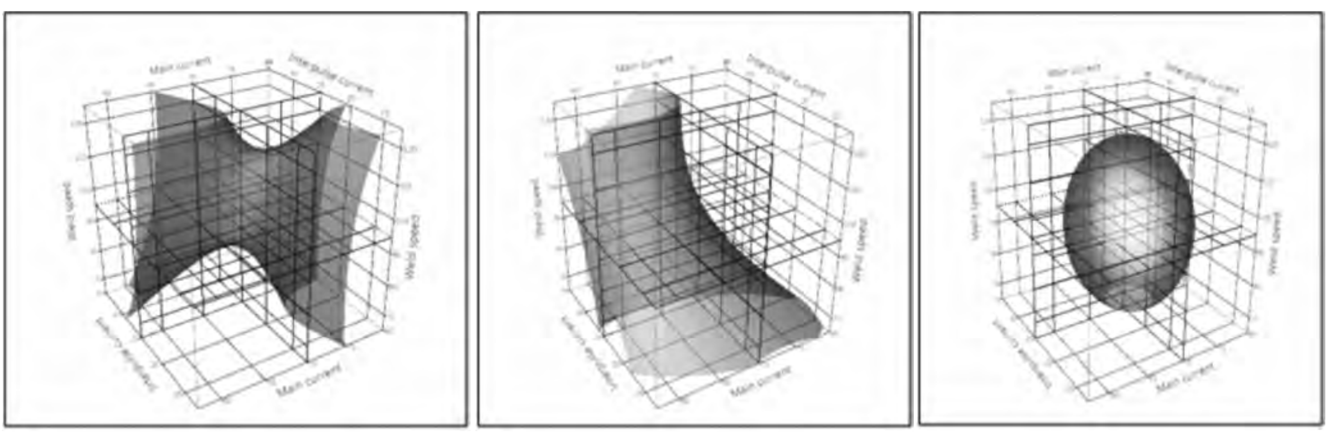

Fig. 7 : Isosurface plot of responses - penetration area, penetration height, HAZ area

5.0 VALIDATION OF DEVELOPED RELATIONSHIP

The confirmatory experiments were conducted with the optimized welding parameters and the results obtained are given below in the **Table 8**. The optimized parameters are; main current 70Amps, delta current 25Amps, welding speed 95 mm/min. The three welded coupons was prepared with the optimized parameter, the weld bead width is reported 4.15mm, reinforcement height 0.14mm, reinforcement area 0.37mm^2, penetration area 3.94mm^2, penetration height 1.28mm, HAZ area 1.01mm^2 and the measured heat input is 181j/mm.

Table 8 : Conformance of optimized parameter

● Main current - 70 Amps	InterPulse current - 25 Amps	Welding speed - 95mm/min
● By experiment	Weld bead width - 4.15mm	
● By predicted	Model weld bead width - 3.96mm	Error in prediction - 4.79%
● By experiment	Reinforcement height - 0.14mm	
● By predicted model	Reinforcement height - 0.15mm	Error in prediction - 7.14%
● By experiment	Reinforcement area - 0.37mm	
● By predicted model	Reinforcement area - 0.36mm	Error in prediction - 2.77%
● By experiment	Penetration area - 3.94mm	
● By predicted	Model penetration area - 3.86mm	Error in prediction - 2.07%
● By experiment	Penetration height - 1.28mm	
● By predicted	Model penetration height - 1.26mm	Error in prediction - 1.59%
● By experiment	HAZ area - 1.01mm	
● By predicted	Model HAZ area - 1.19mm	Error in prediction - 17.82%

6.0 CONCLUSION

An empirical relationship was developed to predict the desired quality of the weld bead. As the error between experimental value and predicted value is very less so the regression model is appropriate and valid. Hence the developed relationship can be effectively used to predict the weld bead width, reinforcement height and area, penetration height and area, HAZ area of Interpulse gas tungsten constricted arc welding process of Titanium alloy (Ti-6Al-4V) at 95% confidence level. The optimized value of process parameters is main current 70Amps, delta current 25Amps and welding speed 95mm/min. The optimum response values obtained are weld bead width 4.15mm, reinforcement height 0.14mm, reinforcement area 0.37mm^2, penetration area 3.94mm^2, penetration height 1.28mm, HAZ area 1.01mm^2. It has been observed that there is a combined effect of the main as well as delta current and welding speed on weld bead geometry and HAZ area. The welding speed has the major effect on the weld bead.

REFERENCES

[1] Balasubramanian M, Jayabalan V and Balasubramanian V (2010); Effect of process parameters of pulsed current tungsten inert gas welding on weld pool geometry of titanium welds, ACTA Metallurgica Sinica, 23(4), pp.312-320.

[2] Davies AC (1984); The Science and Practice of Welding, Volume 1 & 2, 8th edition, Cambridge University Press, Cambridge, London.

[3] Obermiller DJ, Multiple Response Optimizations Using JMP, The Dow Chemical Company, Midland, MI.

[4] Rodrfguez-Carmona E, Manresa A and Bastida J (2013); Application of experimental design, canonical analysis of response surface to the optimization of poly production by Pseudomonas aeruginosa 42A2, Chemical & Biomedical Engineering Quarterly, 27(4), pp.457-465.

[5] Khanna OP (2010); A Text Book of Welding Technology, 19th edition, Dhanpat Rai Publications (P) Ltd., New Delhi.

[6] Kiaee N and Aghaie-Khafri M (2014); Optimization of gas tungsten arc welding process by response surface methodology, Materials and Design, 54, pp.25-31.

[7] Kumar K, Chattopadhyaya S and Yadav A (2012); Surface response methodology for predicting the output responses of TIG welding process, IJMST, 6(2), pp.163-169.

[8] Kumar NP, Bhaskar Y, Mastanaiah P and Murthy CVS (2014); Study on dissimilar welding of 15CDV6 and SAE 4130 steels by Interpulse tungsten arc welding, Procedia Materials Science, 5, pp.2382-2391.

[9] Montgomery DC (1991); Design and Analysis of Experiments, 3rd edition, John Wiley & Sons, New York, USA.

[10] Leary RK, Merson E and Birmingham K (2010); Microstructural and microtextural analysis of interpulse GTCAW welds in Cp-Ti and Ti-6Al-4V, Materials Science and Engineering A, 527, pp.7934-7705.